Crystal Structure and Thermodynamics of Reversible Molecular Capsules

Robert G. Chapman, Gunnar Olovsson, James Trotter, and John C. Sherman*

Contribution from the Department of Chemistry, University of British Columbia, Vancouver, BC, Canada V6T 1Z1

Received January 6, 1998. Revised Manuscript Received April 24, 1998

Abstract: The reversible encapsulation of small molecules by two rigid hemispherical molecules is described. The "bowls" are linked by four charged hydrogen bonds. The complex is highly guest-selective. A crystal structure of one complex and a thermodynamic analysis of several complexes provide an unusually vivid description of the structure and dynamics of these complexes. The relevance of these complexes as transition state models for the formation of carceplexes is also presented.

Introduction

The reversible encapsulation of molecules is fast becoming an important field within supramolecular chemistry.[1] In addition to its broad relevance to molecular recognition in natural and nonnatural systems, reversible molecular encapsulation holds great promise for areas such as drug delivery[2] and molecular sensors.[3] Of utmost importance is having a well-defined system that is highly characterizable. Such a system allows an elucidation of the noncovalent interactions that govern its formation and has great potential for the construction of larger and/or more complex assemblies. We report here a detailed characterization of a reversible complex (**3**•guest) that is highly guest-selective (Scheme 1). In addition, the relevance of complex **3**•guest to the formation of carceplex **2**•guest (Scheme 1) is discussed.

Carceplexes are closed surface compounds that incarcerate smaller molecules or ions.[4] In the formation of carceplex **2**•guest,[5] two molecules of tetrol **1** wrap around a guest/template molecule and the two "bowls" get sown together by the formation of four OCH_2O bridges. This irreversible process is highly efficient, but only works if a suitable template molecule is present.[5] The abilities of template molecules to form carceplex **2**•guest vary by 10^6-fold.[6] The ability of one template versus another to form carceplex **2**•guest is called a *template ratio*. For a series of molecules, the template ratios reflect the relative rates of the guest-determining step (GDS,[7] the step beyond which the guest no longer exchanges under the reaction conditions) for that series of guest molecules. This step is 10^6-times faster in the presence of pyrazine (the best template) than in the presence of *N*-methylpyrrolidinone (NMP, the poorest template). Alternatively, the transition state for the GDS is 8.3 kcal/mol lower in the presence of pyrazine than in the presence of NMP at 300 K.[6]

The GDS for formation of carceplex **2**•guest was determined to be the formation of the second OCH_2O bridge.[6b] Although we cannot study the transition state of this step directly, we can study the ground-state complexation of the immediate precursor to the GDS, the singly bridged intermediate. Even simpler, we can study the ground-state complexation of tetrol **1** with various guest molecules, as the stability of these complexes has been shown to correlate with the template ratios for the formation of carceplex **2**•guest.[8] Thus, this complex is a good transition state model for the GDS in the formation of carceplex **2**•guest. We report here a detailed analysis of complex **3**•guest, including a thermodynamic analysis of the complex in two solvents, and a crystal structure of complex **3**•pyrazine.

Results and Discussion

Characterization of Complex 3•Pyrazine in Solution. The ^{1}H NMR spectrum (spectrum A, Figure 1) of a solution of tetrol

(1) (a) Conn, M. M.; Rebek, J., Jr. *Chem. Rev.* **1997**, *97*, 1647−1688 and references therein. (b) Valdéz, C.; Spitz, U. P.; Toledo, L. M.; Kubik, S. W.; Rebek, J., Jr. *J. Am. Chem. Soc.* **1995**, *117*, 12733−12745. (c) Valdéz, C.; Toledo, L. M.; Spitz, U.; Rebek, J., Jr. *Chem Eur. J.* **1996**, *2*, 989−991. (d) Chapman, R. G.; Sherman, J. C. *Tetrahedron*, **1997**, *53*, 15911−15946 and references therein. (e) Mogck, O.; Pons, M.; Böhmer, V.; Vogt, W. *J. Am. Chem. Soc.* **1997**, *119*, 5706−5712. (f) Mogck, O.; Paulus, E. F.; Böhmer, V.; Thondorf, I.; Vogt, W. *J. Chem. Soc., Chem. Commun.* **1996**, 2533−2534. (g) MacGillivray, L. R.; Atwood, J. L. *Nature* **1997**, *389*, 469−472. (h) Jacopozzi, P.; Dalcanale, E. *Angew. Chem., Int. Ed. Engl.* **1997**, *36*, 613−615. (i) Miklis, P.; Çagin, T.; Goddard, W. A. *J. Am. Chem. Soc.* **1997**, *119*, 7458−7462. (j) Lee, S. B.; Hong, J.-I. *Tetrahedron Lett.* **1996**, *37*, 8501−8504. (k) For a "lidded cucurbituril", including a crystal structure that shows an encapsulated THF molecule, see: Jeon, Y.-H.; Kim, J.; Whang, D.; Kim, K. *J. Am. Chem. Soc.* **1996**, *118*, 9790−9791. See also: Vögtle, F. et al. *Liebigs Ann.* **1996**, 1697−1704.

(2) (a) Aigner, A.; Wolf, S.; Gassen, H. G. *Angew. Chem., Int. Ed. Engl.* **1997**, *36*, 24−41. (b) Lasic, D. D.; Papahadjopoulos, D. *Science* **1995**, *267*, 1275−1276.

(3) (a) Diamond, D.; McKervey, M. A. *Chem. Soc. Rev.* **1996**, 15−24. (b) Kropf, M.; Joselevich, E.; Dürr, H.; Willner, I. *J. Am. Chem. Soc.* **1996**, *118*, 655−665. (c) Zhou, Q.; Swager, T. M. *J. Am. Chem. Soc.* **1995**, *117*, 12593−12602.

(4) Cram, D. J.; Karbach, S.; Kim, Y. H.; Baczynskyj, L.; Marti, K.; Sampson, R. M.; Kalleymeyn, G. W. *J. Am. Chem. Soc.* **1988**, *110*, 2554−2560.

(5) Sherman, J. C.; Knobler, C. B.; Cram, D. J. *J. Am. Chem. Soc.* **1991**, *113*, 2194−2204.

(6) (a) Chapman, R. G.; Chopra, N.; Cochien, E. D.; Sherman, J. C. *J. Am. Chem. Soc.* **1994**, *116*, 369−370. (b) Chapman, R. G.; Sherman, J. C. *J. Org. Chem.* In press.

(7) Abbreviations: GDS, guest determining-step (the GDS is also the product-determining step; we use GDS because our focus is on the guest or template effect in the assembly process; just as a product ratio reflects the relative rates of a product-determining step, in our system, the template ratios reflect the relative rates of the GDS); NMP, *N*-methylpyrrolidinone; DBU, 1,8-diazabicyclo[5.4.0]undec-7-ene; CHB, charged hydrogen bond; $\Delta\delta$, the difference in chemical shifts, usually between free and entrapped guests; DMA, dimethylacetamide; TBA, tetrabutylammonium; CPK, Corey-Pauling-Koltun.

(8) Chapman, R. G.; Sherman, J. C. *J. Am. Chem. Soc.* **1995**, *117*, 9081−9082.

S0002-7863(98)00081-X CCC: $15.00
Published on Web 06/11/1998

Scheme 1

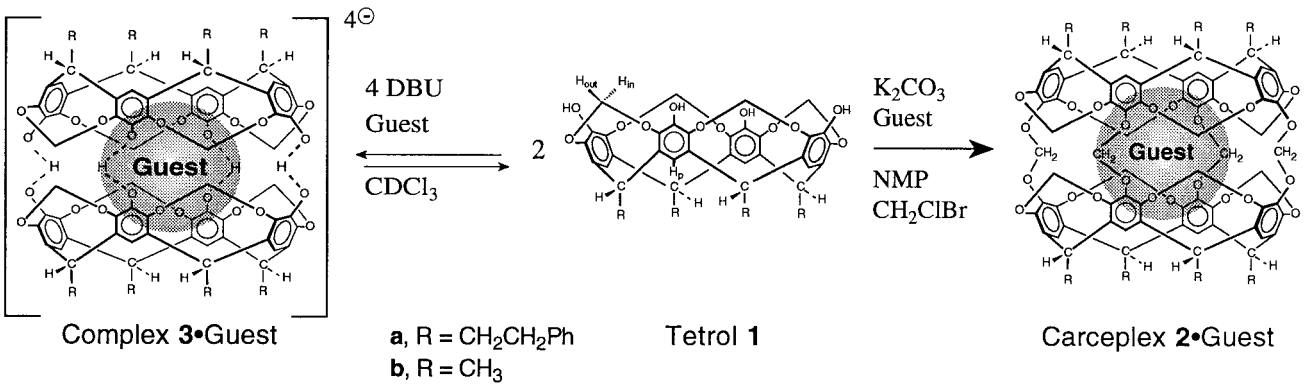

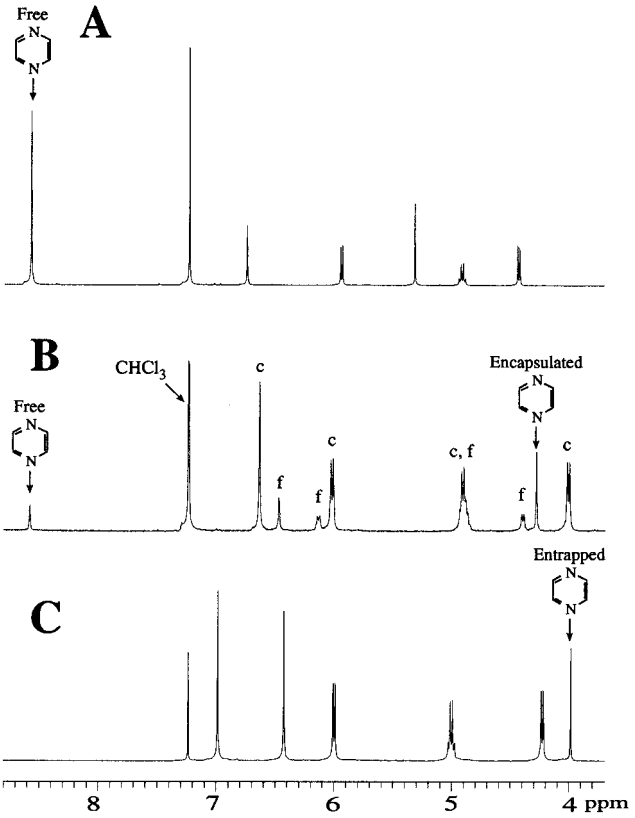

Figure 1. ^{1}H NMR spectra of complex **3b**•pyrazine. ^{1}H NMR spectra in $CDCl_3$ at ambient temperature of (A) Tetrol **1b** (3.7 mM); (B) Tetrol **1b** (3.7 mM), pyrazine (1.9 mM), and DBU (7.8 mM); and (C) carceplex **2b**•pyrazine (8.0 mM). In spectrum B, the host signals assigned to complex **3b**•pyrazine are labeled "c" while the host signals assigned to the "free" species are labeled "f". The signals for CH_3 at ~1.7 ppm for all spectra are not shown. Specific proton assignments for complex **3**•pyrazine are given in the Experimental Section.

1b and 0.50 equiv of the best template molecule for formation of carceplex **2**•guest, pyrazine, in $CDCl_3$ showed no change in the chemical shifts of the host or the guest signals when compared to the ^{1}H NMR spectrum of tetrol **1b** and pyrazine run separately. Thus, there is no complex formed between neutral tetrol **1b** and pyrazine in $CDCl_3$. Addition of 1,8-diazabicyclo-[5.4.0]undec-7-ene (DBU), however, results in two sets of host and guest signals in slow exchange on the ^{1}H NMR time scale at ambient temperature as shown in Figure 1, spectrum B. The necessity of DBU to form this complex suggests that charged hydrogen bonds (CHB's) form between the two bowls. Most apparent in spectrum B is the appearance of a signal for encapsulated pyrazine at 4.3 ppm which is shifted 4.3 ppm upfield from free pyrazine (8.6 ppm). This 4.3 ppm upfield $\Delta\delta$[7] correlates with the 4.6 ppm upfield $\Delta\delta$ observed for incarcerated pyrazine ($\delta = 4.0$ ppm) in carceplex **2b**•pyrazine (spectrum C, Figure 1). Also noticeable in spectrum B is the appearance of two sets of host signals, indicating that both host and guest are in slow exchange on the ^{1}H NMR time scale. Furthermore, integration of the host and guest signals of complex **3b**•pyrazine leads to the expected 2:1 stoichiometry for tetrol **1b**:pyrazine. The ^{1}H NMR data strongly suggest that the structure of complex **3b**•pyrazine is a dimer of tetrol **1b** interconnected by CHB's with a molecule of pyrazine encapsulated within its interior, as illustrated in Scheme 1.

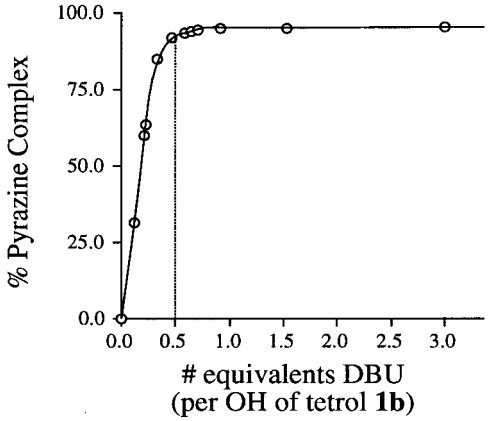

Figure 2. Titration of tetrol **1b** and pyrazine with DBU.

In an effort to evaluate the number of equivalents of DBU that are required for formation of complex **3b**•pyrazine, a titration with DBU was performed on a solution of tetrol **1b** (4.0 mM) and pyrazine (8.0 mM) in $CDCl_3$ and the results were followed by ^{1}H NMR spectroscopy. Integration of the resulting spectra indicates that 0.5 equiv of DBU per phenolic hydroxyl of tetrol **1b** are required to reach the maximum yield of complex **3b**•pyrazine (Figure 2). We therefore conclude that two molecules of tetrol **1b** dimerize around the guest via the formation of $O^-\cdots H-O$ CHB's (Scheme 1). Additionally, the titration experiment suggests that the formation of complex **3b**•pyrazine is highly cooperative, since the ^{1}H NMR spectra of pyrazine and tetrol **1b** with less than a stoichiometric amount of DBU is composed of only two species, complex **3b**•pyrazine and a "free" species; i.e., no intermediates are observed.

No signal for the CHB's was observed in the ^{1}H NMR spectra at 298 K in $CDCl_3$. At 215 K, the ^{1}H NMR spectrum of tetrol **1b** (5.5 mM), pyrazine (2.8 mM), and DBU (11.6 mM) exhibited a new peak at 13.6 ppm that integrated for eight protons per total complex. This was assigned as the fast exchanging average

between the CHB's of tetrol **1b** and the protonated DBU counterion (i.e., DBU•H^+). Tetrabutylammonium (TBA) hydroxide was chosen as the base to eliminate the possibility of proton exchange between complex **3b**•pyrazine and its counterions. The resultant complex, [**3b**•pyrazine][TBA]$_4$, was kinetically stable as it exchanged its guest (more on guest exchange later) over a period of hours at ambient temperature in acetone-d_6, CD_3CN, $CDCl_3$, and DMSO-d_6. The ^{1}H NMR spectrum of complex [**3b**•pyrazine][TBA]$_4$ in acetone-d_6 at 200 K showed a new signal at 15.6 ppm, which was assigned to the CHB's on the basis of its integration for four hydrogens per complex.[9] The large downfield shift indicates that the CHB's connecting the bowls are strong hydrogen bonds.[10,11]

Electrospray ionization mass spectrometry (ESI) of kinetically stable complex [**3b**•pyrazine][TBA]$_4$ in acetonitrile resulted in the detection of a series[12] of signals which included complex **3b**•pyrazine. It is noteworthy that doubly charged complexes (i.e., those with only two CHB's) are detected by ESI;[13] we have discovered related species that contain two CHB's and are stable in solution, which will be reported shortly.[14]

We investigated the orientation and mobility of pyrazine within complex **3b**•pyrazine using a method developed recently.[15] Thus, the ^{1}H NMR spectrum of a mixture of tetrol **1a** (4.12 mM), tetrol **1b** (4.26 mM), DBU (24.0 mM), and pyrazine (21.0 mM) in nitrobenzene-d_5 at ambient temperature yields signals for encapsulated pyrazine represented by a statistical mixture of complex **3a**•pyrazine, complex **3b**•pyrazine, and asymmetric complex **3c**•pyrazine in a 1:2:1 ratio, respectively. The signals for pyrazine in asymmetric complex **3c**•pyrazine consisted of two *meta*-split doublets at 4.31 ($J = 1$ Hz) and 4.35 ppm ($J = 1$ Hz).[16] This confirms that pyrazine is oriented in complex **3b**•pyrazine with its nitrogens at the equator and its hydrogens extending into the bowls (structure **A**, Figure 3). The activation energy for rotation of pyrazine about the pseudo-C_2 axes in asymmetric complex **3c**•pyrazine was measured by variable-temperature ^{1}H NMR spectroscopy to be 18 kcal/ mol,[17] which agrees well with the 19 kcal/mol activation barrier measured in carceplex **2c**•pyrazine (in these systems, a hydrogen appears to be larger than a nitrogen lone pair).[8] Thus

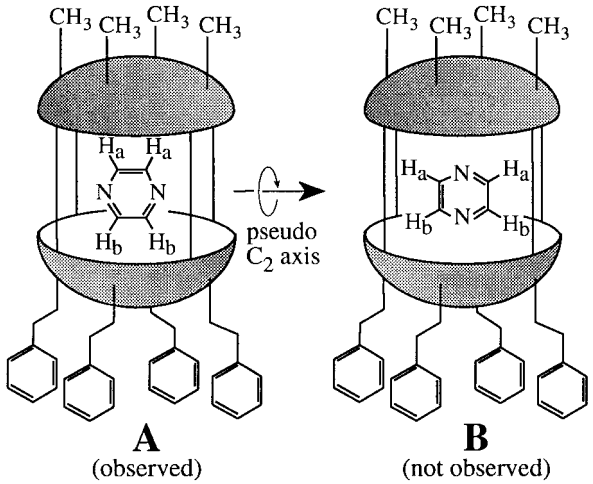

Figure 3. Orientation of pyrazine. Schematic representation of asymmetric carceplex **2c**•pyrazine and complex **3c**•pyrazine. The vertical lines connecting the two bowls represent OCH_2O bonds and CHB's for asymmetric carceplex **2c**•pyrazine and complex **3c**•pyrazine, respectively.

pyrazine has the same orientation and mobility within complex **3**•pyrazine and carceplex **2**•pyrazine.

Characterization of Complex 3•Pyrazine in the Solid State. Light yellow crystals of complex **3b**•pyrazine were grown in nitrobenzene from a mixture of tetrol **1b** (14 mM), DBU (28 mM), and pyrazine (114 mM). A stereoview that shows the orientation of pyrazine is shown in Figure 4. Only one of the two degenerate orientations of pyrazine is displayed in Figure 4 (see Experimental Section). The unit cell contains two crystallographically unique assemblies of complex **3b**•pyrazine which differ only in the direction of the chiral twist of the upper and lower bowls with respect to each other. Figure 5 is a partial view of the packing diagram, which shows that each complex is surrounded by four DBU•H^+ counterions. In the solid state, all four DBU•H^+ counterions are coordinated to the same bowl in a given complex; i.e., they do not alternate on top and bottom bowls. The DBU•H^+ ions are hydrogen bonded to the phenoxide oxygen that is more distant from the O−H---O^- hydrogen. The CHB O···O distance is 2.59 Å, which is indicative of strong O−H---O^- hydrogen bonds.[10] The O···N distance is 2.74 Å, which is characteristic of strong N−H---O hydrogen bonds.[10, 18]

The most obvious observation one can make from the crystal structure of complex **3b**•pyrazine is that the pyrazine is encapsulated within the interior of two bowls, which are connected to each other by four CHB's. Pyrazine sits with its nitrogens along the equator and its hydrogens extending into the aromatic cavity of the bowls as shown in solution by ^{1}H NMR spectroscopy (vide supra). To the best of our knowledge, this is the first structure of a reversible molecular capsule that unambiguously reveals the presence of and, what is more, the orientation of an encapsulated guest molecule.[1b,c,f,g,k]

The crystal structures of complex **3b**•pyrazine and carceplex **2b**•pyrazine show some remarkable similarities. In fact, the only major difference between the two is the noncovalent bonds

(9) The CHB protons readily exchange with a deuterium from acetone-d_6 or residual D_2O present in the NMR solvent. After a period of a few hours the CHB signal would completely disappear even at 200 K; addition of a tiny amount of H_2O to this sample, however, regenerated this signal. Therefore, a more accurate integration for the CHB of complex [**3b**•pyrazine]-[TBA]$_4$ was achieved by adding the solid complex, [**3b**•pyrazine][TBA]$_4$, to a ^{1}H NMR tube containing acetone-d_6 with 10 additional equivalents of pyrazine, and this sample was allowed to equilibrate for only 10 min in the ^{1}H NMR spectrometer at 200 K before acquisition of the spectrum.

(10) (a) Hibbert, F.; Emsley, J. *Adv. Phys. Org. Chem.* **1990**, *26*, 255−379. (b) Emsley, J. *Chem. Soc. Rev.* **1980**, *9*, 91−124.

(11) The chemical shift of the CHB protons was highly sensitive to small amounts of water (the sample was run containing molecular sieves, which catalyze H/D exchange with acetone as well as the condensation of acetone, which generates more water). Thus, the $\Delta\delta$ of protons versus deuterons, which is an indication of hydrogen bond strength, was not possible. See: (a) Cleland, W. W. *Biochemistry* **1992**, *31*, 317−319. (b) Smirnov, S. N.; Golubev, N. S.; Denisov, G. S.; Benedict, H.; Schah-Mohammedi, P.; Limbach, H.-H. *J. Am. Chem. Soc.* **1996**, *118*, 4094−4101.

(12) See Supporting Information. Counterion exchange from TBA to H^+ further complicated the spectrum.

(13) The doubly charged bis-bowl species observed by ESI have some kinetic stability, but are not likely to be thermodynamically stable enough to be observed in solution, according to the data presented in Figure 2.

(14) Chapman, R. G.; Sherman, J. C. Manuscript in preparation.

(15) Fraser, J. R.; Borecka, B.; Trotter, J.; Sherman, J. C. *J. Org. Chem.* **1995**, *60*, 1207−1213.

(16) Resolution enhancement of these signals indicated they were coupled, $J = 1$ Hz. Enhancement was done by performing a Gaussian multiplication (GB = 0.5) of the free-induction decay and setting line broadening to −1.

(17) The activation barrier for rotation of pyrazine about the pseudo-C_2 axes of asymmetric complex **3c**•pyrazine was calculated to be 18.3 kcal/mol based on a coalescence temperature (T_c) of 353 K and separation of the signals ($\Delta\delta_{Hz}$) of 14.3 Hz using the following equation: $\Delta G_c^{\ddagger} = RT_c[22.96 + \ln(T_c/\Delta\delta_{Hz})]$ where $\Delta G_c^{\ddagger}$ is the activation barrier in kcal/mol; T_c is the temperature of coalescence, and $\Delta\delta_{Hz}$ is the separation of the signals in Hz. See: Abraham, R. J.; Fisher, J.; Loftus, P. *Introduction to NMR Spectroscopy*; Wiley: New York, 1990; pp 194−197.

(18) Novak, A. *Struct. Bonding* **1974**, *18*, 177−216.

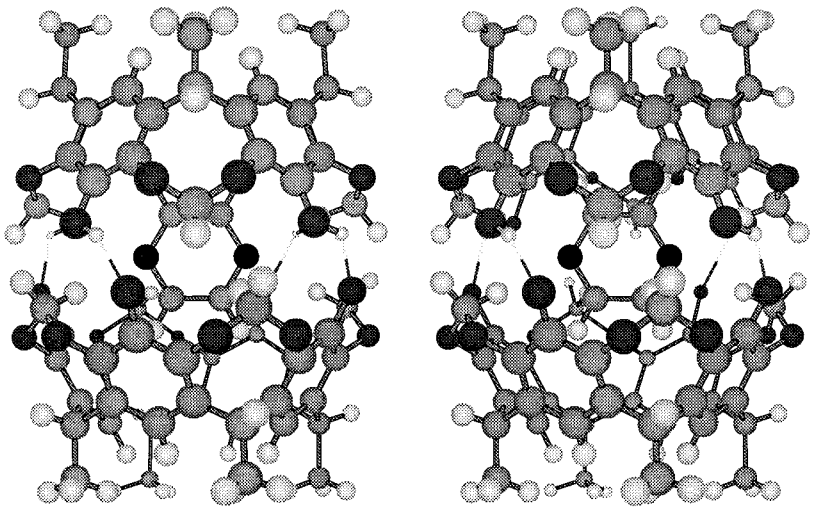

Figure 4. Stereoview of the crystal structure of complex **3b**•pyrazine.

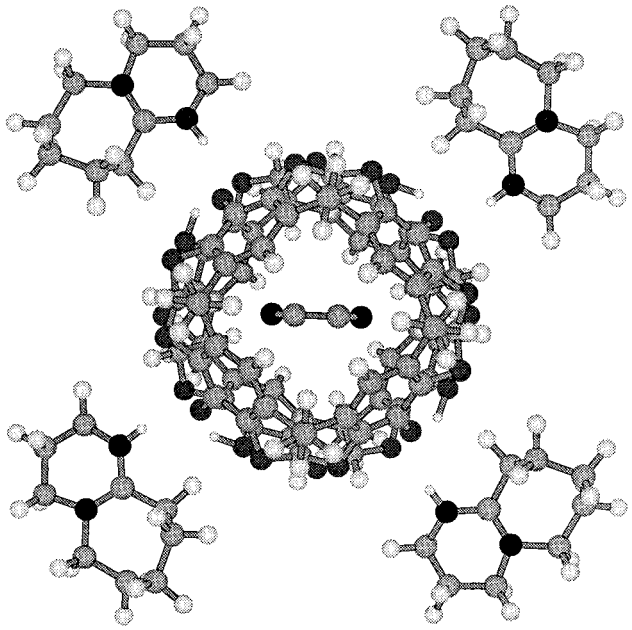

Figure 5. Partial packing diagram for [complex **3b**•pyrazine]-[DBU•H^+]$_4$.

that connect the bowls of complex **3b**•pyrazine versus the covalent bonds that connect the bowls of carceplex **2b**•pyrazine. Therefore, the remainder of the discussion of the crystal structure of complex **3b**•pyrazine is as a comparison with the crystal structure of carceplex **2b**•pyrazine.

Figure 6 shows two views of the crystal structures of carceplex **2b**•pyrazine and complex **3b**•pyrazine side by side. These views focus on the twist between the bowls (**A**, top view) and the distance between the bowls (**B**, side view). It is evident that pyrazine displays the same orientation in both structures. Furthermore, the bowls are twisted with respect to each other about the C_4 axis by 21.0° and 21.8° for the carceplex and complex, respectively, which allows the ideal torsional angles for conjugation of the aryl ethers or phenols/phenoxides with their respective aromatic rings.[15,19a] The conjugation of eight aryl ethers likely provides 16−24 kcal/mol of stabilization energy.[15,19a] The twist of the bowls also maximizes van der Waals interactions between both the bowls and the guest and between the upper rims of the bowls by providing more close contacts; the twist also reduces steric strain between the opposing methylenes that line the rims of the bowls. Interestingly, in the corresponding carceplex, where the inter-bowl linkages are $-SCH_2S-$ instead of $-OCH_2O-$, the bowls are not twisted with respect to each other, presumably because conjugation of aryl sulfides is very weak.[19b]

The distances between the planes that connect the phenolic oxygens of carceplex **2b**•pyrazine and complex **3b**•pyrazine are 2.23 and 2.43 Å, respectively, indicating that the carceplex is slightly more compressed than the complex. These differences may help explain the slightly higher activation energy barrier for rotation of pyrazine within carceplex **2b**•pyrazine (19 kcal/mol) versus complex **3b**•pyrazine (18 kcal/mol).

In Figure 6, the top view of complex **3b**•pyrazine shows that the nitrogens of pyrazine are not involved in hydrogen bonding with the O−H---O^- hydrogens, as the closest such N---H distance is 3.8 Å. Also, the top view indicates that the nitrogens of pyrazine are involved in weak hydrogen bonds to half of the hydrogens of the intra-bowl methylenes. The closest such N-to-H distances for complex **3b**•pyrazine are 2.32 and 2.48 Å for the lower and upper bowls, respectively, while the closest such N-to-H distances for carceplex **2b**•pyrazine are at 2.41 and 2.64 Å for the lower and upper bowls, respectively. The other half of the methylene bridges (the ones perpendicular to the aromatic ring of the guest) are 3.3−3.5 Å away from the plane of pyrazine, which indicates loose CH−π hydrogen bonds between these hydrogens and the π system of pyrazine.[20] The distances between the hydrogens of pyrazine and the closest aromatic carbon atom of the top and bottom bowls are 2.78 and 2.90 Å for complex **3b**•pyrazine, and 2.73 and 2.90 Å for carceplex **2b**•pyrazine. These close contacts indicate that these hydrogens are close enough to form close CH−π hydrogen bonds.[20]

Guest Selectivity in Complex 3•Guest. We determined the relative stabilities (K_{rel}) of complex **3b**•guest via competition experiments, by integrating the unique host and guest signals in the ^{1}H NMR spectra of mixtures of tetrol **1b**, DBU, guest 1, and guest 2 in $CDCl_3$.[8,21] The results, recorded in Table 1, show that complex **3b**•guest is highly guest selective; this selectivity correlates with the selectivity observed for formation of carceplex **2a**•guest, as a plot of the ln(K_{rel} in $CDCl_3$) versus the ln-

(19) (a) Spellmeyer, D. C.; Grootenhuis, P. D. J.; Miller, M. D.; Kuyper, L. F.; Kollman, P. A. *J. Phys. Chem.* **1990**, *94*, 4483−4491. (b) Helgeson, R. C.; Knobler, C. B.; Cram, D. J. *J. Chem. Soc., Chem. Commun.* **1995**, 307−308.

(20) Nishio, M.; Umezawa, Y.; Hirota, M.; Takeuchi, Y. *Tetrahedron* **1995**, *51*, 8665−8701.

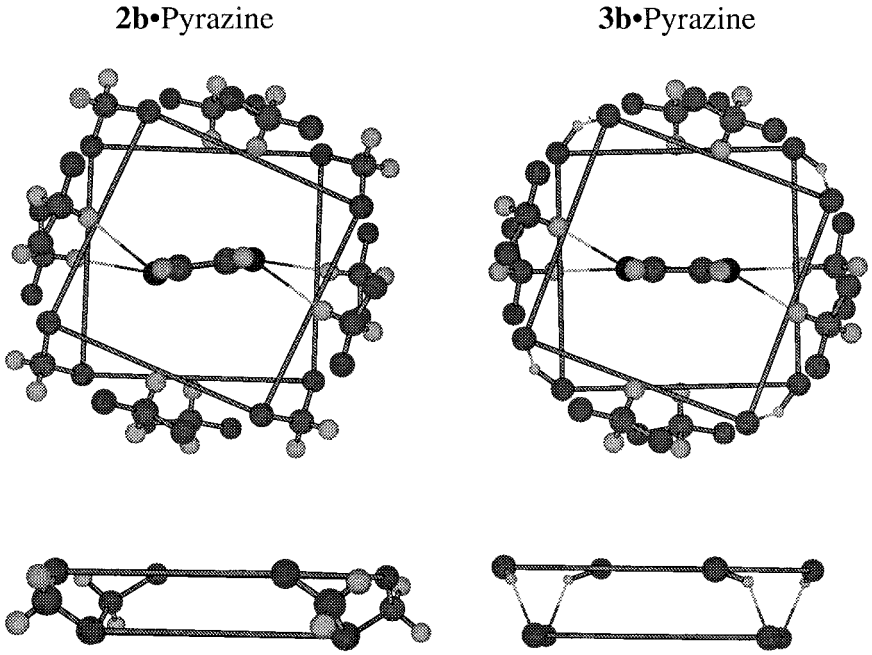

Figure 6. View of the planes connecting the inter-bowl aryl ethers of carceplex **2b**•pyrazine and the phenols/phenoxides of complex **3b**•pyrazine. Partial views of the crystal structures of carceplex **2b**•pyrazine (left) and complex **3b**•pyrazine (right). The planes that connect the aryl ethers of carceplex **2b**•pyrazine and the phenols/phenoxides of complex **3b**•pyrazine are drawn in. The distance between the planes in carceplex **2b**•pyrazine is 2.23 Å as calculated by the 2.36 Å distance from O-to-O and a 21.0° twist of the bowls with respect to each other (cos(21.0) × 2.36 Å = 2.23 Å). Similarly, the distance between the planes in complex **3b**•pyrazine was calculated to be 2.43 Å. In the top views, the close contacts between the N of pyrazine and the intra-bowl methylene C−H's are shown.

Table 1. K_{rel}'s of Complex **3b**•Guest in Nitrobenzene-d_5 and $CDCl_3$ (at 298 K) and Template Ratios for Carceplex **2**•Guest

guest[a]	template ratio[b]	K_{rel} of complex **3b**•guest in nitrobenzene-d_5[c]	K_{rel} of complex **3b**•guest in $CDCl_3$[d]
pyrazine	1 000 000 (860)	980 000 (1800)	1300
methyl acetate	470 000 (−)	420 000 (780)	–
dioxane	290 000 (180)	240 000 (450)	77
DMSO	70 000 (19)	58 000 (110)	14
pyridine	34 000 (14)	7100 (13)	9.6
acetone-d_6	6 700 (2)	1300 (2.4)	0.9
benzene-d_6	2 400 (1)	540 (1)	1
1,3-dioxane	200	140	
DMA	20	8.9	
$CHCl_3$		5.8	
NMP	1	1	
morpholine		38 000	

[a] The K_{rel}'s determined in nitrobenzene-d_5 for complex **3b**•acetone and complex **3b**•benzene used nondeuterated acetone and benzene as guests. [b] The template ratios reported were determined at 60 °C for 2 d or at ambient temperature for 1 d and 2 d at 60 °C, for carceplex **2a**•guest.[6] The template ratios in parentheses were determined at ambient temperature for 2 d for carceplex **2b**•guest, and are normalized to benzene.[8] [c] The numbers in parentheses are normalized to benzene. [d] Data from ref 8; some numbers have been modified after more rigorous analysis of original data.

(template ratios for carceplex **2a**•guest) yields a correlation factor of $r^2 = 0.94$ (a similar plot for data in nitrobenzene-d_5, see Table 1, gives $r^2 = 0.98$). This correlation suggests that the nature of the guest molecule imparts a similar stabilizing or destabilizing effect on the relative free energies of complex **3b**•guest as it does to the relative activation energies of the transition state of the GDS in the formation of carceplex **2a**•guest. This agreement implies that the interactions that govern the formation of both carceplex **2a**•guest and complex **3b**•guest are similar, and therefore, this complex does represent a good transition state model for the GDS in the formation of carceplex **2a**•guest.

(21) The guests acetone and benzene were added as acetone-d_6 and benzene-d_6 so as to not wash out the ^{1}H NMR signals for the host signals of complex **3b**•guest. Guest 1 and guest 2 were added in ratios that yield a ~1:1 ratio of complex **3b**•guest 1:complex **3b**•guest 2, and such that the total amount of free species that remained represented less than 15% of the total concentration of host.

Table 2. Thermodynamic Data for Complex **3b**•Guest in $CDCl_3$ and Nitrobenzene-d_5[a]

guest	$\Delta\Delta H°$, kcal/mol $C_6D_5NO_2$	$T\Delta\Delta S°$,[b] kcal/mol $C_6D_5NO_2$	$\Delta\Delta G°$, kcal/mol $C_6D_5NO_2$	$\Delta\Delta H°$, kcal/mol $CDCl_3$	$T\Delta\Delta S°$,[b] kcal/mol $CDCl_3$	$\Delta\Delta G°$,[b] kcal/mol $CDCl_3$
pyrazine	−3.0	1.4	−4.4	−1.2	3.1	−4.3
methyl acetate	−2.8	1.1	−3.9			
dioxane	−4.7	−1.1	−3.6	−1.2	1.5	−2.7
DMSO	0.8	3.6	−2.8	7.1	8.7	−1.7
pyridine	−0.8	0.7	−1.5	0.6	1.9	−1.4
acetone	0.8	1.3	−0.5	4.9	4.9	0.0
benzene	0.0	0.0	0.0	0.0	0.0	0.0

[a] Errors are estimated to be ±20%. [b] Temperature = 300 K.

Thermodynamics of Complex 3•Guest in $CDCl_3$. We determined the temperature dependence of the relative stabilities of complex **3**•guest in $CDCl_3$ with six guest molecules. A van't Hoff plot of the data (from 253 to 323 K, $r^2 = 0.99$ for all data) generated the relative enthalpies and entropies as well as the relative free energies for these complexes, which are given in Table 2; benzene was arbitrarily chosen as a reference point and set to zero for simplicity. In these experiments, it was critical to ensure that the samples had reached equilibrium. The amount of time necessary to reach equilibrium in the competition experiments depended greatly on temperature and on the guest encapsulated in complex **3b**•guest. We determined the time necessary to achieve equilibrium by two different methods: (1) simply recording the ^{1}H NMR spectrum over time until no change was observed or (2) waiting five times the calculated half-life for the decomplexation rate of our best guest, pyrazine.[22]

Table 2 shows that small changes in guest molecules are manifested by large perturbations to the energetics of the complex. For example, pyrazine and pyridine differ only by the substitution of a CH group with nitrogen, but the relative free energies of their complexes differ by 2.2 kcal/mol at 300 K. This difference is not likely to be due to hydrogen bonding of the encapsulated guest molecule with the CHB's of the complex, as there is no evidence for such interactions in the crystal structure of complex **3b•**pyrazine, nor due to the charge of the guest molecule itself as both pyridine and pyrazine bear the same charge. In addition, the strong correlation between the template ratios of carceplex **2a•**guest determined in NMP ($\epsilon_r = 32.2$)[23] and the K_{rel}'s determined in $CDCl_3$ ($\epsilon_r = 4.8$)[23] and in nitrobenzene-d_5, (vide infra, $\epsilon_r = 34.8$)[23] suggest that solvation is not a significant component of the observed selectivity. Examination of the relative enthalpic and relative entropic components of all six complexes **3b•**guest provides for a more detailed picture of the driving forces for complex **3b•**guest.

The enthalpic component of the stabilities of the complexes is undoubtedly composed of a variety of noncovalent interactions including van der Waals, electrostatic, and $\pi-\pi$ interactions as well as hydrogen bonding such as O−H---O$^-$ and CH$-\pi$. DMSO and acetone complexes are the least favored enthalpically, most likely because of their size and shape, which provide poor van der Waals and CH$-\pi$ interactions, and no $\pi-\pi$ interactions with the interior of the complex, according to CPK[7] models. Pyrazine and dioxane complexes are the most enthalpically favored guests, which is interesting considering the similarity of their shapes. Examination of CPK models and the crystal structure of complex **3b•**pyrazine reveals that (1) both pyrazine and dioxane form highly favorable van der Waals interactions with the interior walls of the complex, (2) both guests can form CH$-\pi$ hydrogen bonds with the arenes of the bowls, and (3) both guests can form CH−X hydrogen bonds between their heteroatoms and the inward-pointing intra-bowl acetal (OCH_2O) hydrogens. However, only pyrazine can participate in CH$-\pi$ hydrogen bonds with the remaining inward-pointing (OCH_2O) hydrogens of the bowls, and form $\pi-\pi$ interactions with the electron-rich arenes of the bowls. That both pyridine and benzene complexes are less favored enthalpically compared to pyrazine could be due to the larger guests being less complementary to the interior of the host as suggested by CPK models (vide supra and see ref 8 for the size of hydrogen versus a nitrogen lone pair). Such steric strain could cause a partial unraveling of the twist between the bowls, which could weaken the O−H---O$^-$ CHB's and diminish the conjugation of the aryl ethers. Additionally, the lower enthalpy of benzene and pyridine could be due to the loss of one CH−X hydrogen bond between the heteroatom of the guest and the inward-pointing (OCH_2O) hydrogens of the bowls in the case of pyridine, and all such bonds in the case of benzene. Complex **3b•**pyridine is less favored enthalpically compared to both complexes **3b•**pyrazine and **3b•**benzene, possibly because, unlike pyrazine and benzene, pyridine has a substantial dipole moment. Complex **3b** does not have a dipole moment because of its symmetry, thus it may favor guests that also do not have a dipole (pyrazine and benzene) over guests that do (pyridine).

Complexes **3b•**guest have a large favorable entropic component with respect to complex **3b•**benzene. For example, the formation of complex **3b•**DMSO and complex **3b•**acetone are strongly favored entropically relative to benzene. This is most likely a result of the relatively small size of acetone and DMSO, which allow greater mobility of these guests within the interior of the host. Entropy of solvation may also be important and is discussed further below. Benzene forms the least entropically favored complex most likely because its large size restricts its mobility within the interior of the complex and perhaps distorts the bowls and/or the bowl-to-bowl alignment.

Thermodynamics of Complex 3•Guest in Nitrobenzene-d_5. The relative stability constants of complex **3b•**guest at 298 K for several guest molecules in nitrobenzene-d_5 are reported in Table 1. Nitrobenzene allows us to determine K_{rel}'s all the way down to NMP,[7] whereas we must stop at acetone or benzene when using $CDCl_3$.[24,25] The general reproduction of the 10^6-fold range in guest effects found here and in the template ratios (Table 1) suggests that binding is the dominant factor in the transition state of the GDS for formation of carceplex **2•**guest; the rate constants for the reaction to form the second bridge (i.e., the GDS) are likely to be far less dependent on the template molecules. There are some differences observed for the two sets of K_{rel}'s reported in Table 1, but these differences are not significant enough for detailed interpretation. However, the relative enthalpies and entropies are different enough to warrant interpretation (vide infra). It should be noted that the time required to reach equilibrium for determination of the K_{rel}'s in $CDCl_3$ and nitrobenzene-d_5 varies considerably. In $CDCl_3$ equilibration is achieved in minutes at 298 K, while in nitrobenzene-d_5 at 298 K, equilibration takes hours (e.g., $t_{1/2} =$ 1.5 h for the out rate of pyrazine at 296 K; see Experimental Section).

Thermodynamic data were determined in nitrobenzene-d_5 (from 293 to 333 K, $r^2 > 0.94$ for five plots, and 0.87 for one) much the same as they were determined in $CDCl_3$ (vide supra) and are reported in Table 2. There are differences observed for the values of $T\Delta\Delta S°$ and $\Delta\Delta H°$ for complex **3b•**guest in these two solvents, but the same trends still remain. However, some solvent effects are apparent. For example, complex **3b•**pyridine is favored enthalpically relative to complex **3b•**benzene in nitrobenzene-d_5 while the reverse is true in $CDCl_3$. This is most likely due to the different solvation of pyridine and benzene in $CDCl_3$ and nitrobenzene-d_5. These two solvents differ greatly in their polarities (nitrobenzene, $\epsilon_r = 34.8$; $CDCl_3$, $\epsilon_r = 4.8$)[23] and thus one might expect that the solvation enthalpies of such guests would be significantly different. Further analysis of the

(22) The exchange rate of pyrazine is assumed to be the slowest of the guests at all temperatures, and decomplexation is assumed to be the slowest step in achieving equilibrium (i.e., the in-rates of all guests are much faster than the out-rate of pyrazine at all concentrations of guests studied). The decomplexation rate of pyrazine from complex **3b•**pyrazine was shown to be much slower than the decomplexation rates of dioxane or DMSO from complexes **3b•**dioxane and **3b•**DMSO, respectively, at ambient temperature (see Experimental Section).

(23) Reichardt, C. *Solvents and Solvent Effects in Organic Chemistry*, 2nd ed.; VCH: New York, 1988.

(24) The "free" species in $CDCl_3$ is complex **3•**$CDCl_3$ (see ref 8; a detailed description of complex **3•**$CDCl_3$ is in preparation). Since $CDCl_3$ is a weakly competing guest, it limits the guests explored, in neat $CDCl_3$, to the strongest. Nitrobenzene is not a competitive guest; thus, K_{rel} down to NMP can be determined in nitrobenzene-d_5.

(25) Interestingly, morpholine was encapsulated as complex **3b•**morpholine (Table 2). This result contradicts our finding that complex **3b•**guest is a good model for the transition state for formation of carceplexes because carceplex **2a•**morpholine was never isolated. Possible explanations for this are as follows: (1) Morpholine is a sterically demanding guest and may be too large to allow for efficient bridge formation after the GDS; thus polymerization effectively competes against carceplex formation. (2) Morpholine itself could act as a nucleophile from within a carceplex intermediate and attack the chloromethyl ether ($ArOCH_2-Cl$) formed during formation of the methylene bridges (OCH_2O); this would leave a free phenolic hydroxyl that could lead to the formation of polymer. (3) Carceplex **2a•**morpholine was lost during workup due to formation of its $R_2NH_2^+$ salt, which would have remained on the silica gel during column chromatography.

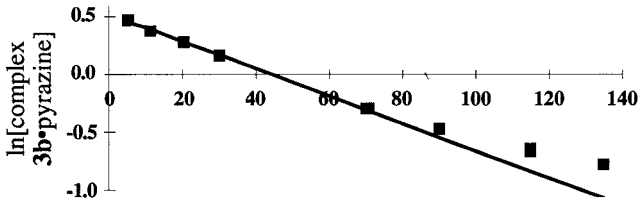

Figure 7. Plot of ln[complex **3b**•pyrazine] versus time at 273 K in $CDCl_3$, $r^2 = 0.99$.

solvation energies of these guest molecules in $CDCl_3$ and nitrobenzene-d_5 may shed light on these data.[26]

In addition to the six guest molecules discussed above (pyrazine, dioxane, DMSO, pyridine, acetone, and benzene), the relative thermodynamic data for complex **3b**•methyl acetate were determined in nitrobenzene-d_5. Examination of a CPK model of complex **3b**•methyl acetate suggests that the guest is highly complementary to the interior of the host and thus should form favorable van der Waals interactions. The methyl groups of the guest in complex **3b**•methyl acetate extend deep into the aromatic cavity and the carbonyl oxygen is positioned such that it can interact with the methylenes that line the equator of the complex. Thus, it is not surprising that complex **3b**•methyl acetate is enthalpically favored relative to complex **3b**•benzene. As well, the overall stability of complex **3b**•methyl acetate corresponds with the template ratios determined for formation of carceplex **2**•methyl acetate.[6b]

pH Switch. Perhaps the most intriguing feature of complex **3b**•guest is that it is formed by noncovalent interactions. This makes it a particularly attractive target for a molecular switch.[27] The titration experiments reported clearly indicate that base is necessary for formation of complex **3b**•guest. Therefore, the neutralization of the base by addition of an acid should destroy complex **3b**•guest and regenerate the free guest and tetrol **1b**. Thus, addition of 1 equiv (3.44 mM) of trifluoroacetic acid (TFA) to a solution of tetrol **1b** (3.44 mM), pyrazine (1.72 mM), and DBU (7.22 mM) at ambient temperature reduced the amount of complex **3b**•pyrazine by one-half. Addition of a further 1.1 equiv of TFA (7.22 mM total) to this sample resulted in the disappearance of all of the pyrazine complex and gave a spectrum that consisted largely of tetrol **1b** and free pyrazine. Addition of more DBU regenerated the complex. Therefore, complex **3b**•guest is indeed pH switchable, which may be a useful property for controlling the release of an encapsulated guest.

Conclusions

We have presented the discovery and characterization of a new family of switchable self-assembling structures. These assemblies are excellent models for studying the importance of noncovalent interactions between molecules, because small changes in guests result in large differences in the relative free energy of binding of these complexes. Moreover, the solution and solid state characterization provide unprecedented detail for such complexes, particularly with respect to the orientation and mobility of the encapsulated guests.

(26) For a computational analysis of complex **3**•guest (calculations were performed on a dimer of tetrol **1** containing no CHB's), including solvation energies of the guests, see: Nakamura, K.; Sheu, C.; Constable, A. E.; Houk, K. N.; Chapman, R. G.; Sherman, J. C. *J. Am. Chem. Soc.* **1997**, *119*, 4321−4322.

(27) (a) Branda, N.; Grotzfield, R. M.; Valdéz, C.; Rebek, J., Jr. *J. Am. Chem. Soc.* **1995**, *117*, 85−88. (b) Bissell, R. A.; Córdova, E.; Kaifer, A. E.; Stoddart, J. F. *Nature* **1994**, *369*, 133−137. (c) Debreczeny, M. P.; Svec, W. A.; Wasielewski, M. R. *Science* **1996**, *274*, 584−587.

Table 3. ^{1}H NMR Assignments for Complexes **3b**•Guest in $CDCl_3$ at 298 K

complex **3b**•guest[a]	H_p	H_{out}	methine	H_{in}	CH_3	guest signals
pyrazine	6.66	6.00	4.90	4.01	1.69	4.30 (s, 4H)
1,4-dioxane	6.50	6.16	4.89	4.27	1.62	0.03 (br, 8H)
DMSO	6.51	6.12	4.87	4.27	1.63	−1.02 (s, 6H)
pyridine	6.66	5.98	4.89	3.99	1.69	6.27 (m, 1H), 4.30 (m, 2H), 3.00 (m, 2H)
acetone-d_6	6.47	6.14	4.87	4.09	1.61	
benzene-d_6	6.74	6.09	4.98	4.12	1.77	
stock solution	6.48	6.14	4.89	4.40	1.63	

[a] See Scheme 1 for designation of H_p, H_{in}, and H_{out}. ^{1}H NMR spectra were all well resolved: H_p (s, 8H), H_{out} (d, $J = 7.2-7.7$ Hz, 8H), methine (m, 8H), H_{in} (d, $J = 7.4-7.7$ Hz, 8H), CH_3 (d, $J = 7.4-7.9$ 24H). The signals for the DBU•H^+ in the stock solution are as follows: 3.44 (m, 2H), 3.26 (m, 6H), 2.67 (m, 2H), 1.85 (m, 2H), 1.70 (m, 2H), 1.56 (m, 2H).

The strong correlation between template ratios for formation of carceplex **2a**•guest and relative stabilities of complexes **3b**•guest suggests that the favorable noncovalent interactions that govern the formation of complex **3**•guest play an integral role in the stabilization of the transition state for formation of carceplex **2**•guest (i.e., complex **3b**•guest is an excellent transition state model for the GDS in the formation of carceplex **2a**•guest). These interactions include CHB's between the bowls, van der Waals interactions between both the guest and the interior of the complex as well as between the upper rims of the bowls themselves, CH$-\pi$ interactions between both the hydrogens of the guest with the arenes of the bowls and the hydrogens of intra-bowl methylene bridges with the guest, CH$-$X hydrogen bonding between the hydrogens of the intra-bowl methylene bridges of the bowls to the guest, conjugation of the O$-$H---O$^-$ and OCH_2O bonds into their respective aromatic rings, and $\pi-\pi$ interactions between the arenes of the bowls and the guest.

Evaluation of the enthalpic and entropic components of the free energy of the complexes allows a more in-depth analysis of the noncovalent interactions that drive their formation. Relative thermodynamic data were determined for complex **3b**•guest with six guest molecules in both $CDCl_3$ and nitrobenzene-d_5. Guest molecules with the best apparent van der Waals interactions were generally enthalpically favored relative to those guests that provide poor van der Waals interactions; in terms of entropy, small guest molecules that could have substantial mobility within the interior of the complex were found to be favored relative to larger, more sterically demanding guests.

With respect to solvation, the correlation of the relative stability constants of complex **3b**•guest in $CDCl_3$ and nitrobenzene-d_5 with the template ratios determined for the formation of carceplex **2a**•guest in NMP suggests that solvation is not very important in terms of the free energy of the complexes. The relative thermodynamic data determined in $CDCl_3$ for complex **3b**•guest differed slightly from that determined in nitrobenzene-d_5; thus the enthalpy and entropy of solvation of guest molecules in these two solvents must differ. In addition to providing information about solvent effects on the formation of complex **3**•guest, the use of nitrobenzene as solvent also allows the determination of apparent stability constants, which will be reported shortly.

Assemblies such as complex **3b**•guest and carceplex **2a**•guest are excellent systems for theoretical analysis due to their high sensitivity to small perturbations. The energies calculated for complex **3b**•guest reproduced the trend observed for the tem-

Table 4. ^{1}H NMR Assignments for Complex **3b**•Guest in Nitrobenzene-d_5 at 298 K

complex **3b**•guest[a]	H_p	H_{out}	H_{in}	guest signals
pyrazine	7.26 (s, 8H)	6.80 (d, 8H)	4.82 (d, 8H)	5.04 (s, 4H)
methyl acetate	7.06 (s, 4H) 7.05 (s, 4H)	6.94 (m, 8H)	4.87 (d, 8H)	0.04 (s, 3H), −1.50 (s, 3H)
1,4-dioxane[b]	7.10 (s, 8H)	6.97 (d, 8H)	5.08 (d, 8H)	0.79 (br, 8H)
DMSO[b]	7.12 (s, 8H)	6.88 (d, 8H)	5.05 (d, 8H)	−0.29 (s, 6H)
pyridine	7.27 (s, 8H)	6.79 (d, 8H)	4.79 (d, 8H)	7.01 (m, 1H), 5.04 (m, 2H), 3.72 (m, 2H)
acetone	7.10 (s, 8H)	6.95 (d, 8H)	4.91 (d, 8H)	−0.67 (s, 6H)
benzene	7.26 (s, 8H)	6.74 (d, 8H)	4.81 (m, 8H)	4.75 (s, 6H)
1,3-dioxane	7.10 (s, 8H)	6.93 (d, 8H)	5.18 (d, 8H)	−1.28 (br, 2H)[c]
DMA[d]	7.10 (s, 8H)	6.85 (d, 8H)	5.15 (m, 8H)	−0.56 (s, 3H), −1.51 (s, 3H)[c]
$CHCl_3$[d]	7.08 (s, 8H)	6.95 (d, 8H)	5.23 (d, 8H)	5.41 (s, 1H)
NMP[d]	7.09 (s, 4H) 7.06 (s, 4H)	6.74 (d, 8H)	5.02 (br, 8H)	−0.72 (br, 1H), −0.89 (br, 4H), −1.22 (br, 1H), −1.36 (br, 1H)[c]
morpholine	7.10 (s, 8H)	6.91 (d, 8H)	5.16 (m, 8H)	(br, 2H), 0.78 (br, 2H), 0.63 (br, 2H), 0.26 (br, 1H), −0.11 (br, 2H), −0.20 (br, 2H)
stock solution	7.08 (br, 16H)	H_p and H_{out}	4.66 (br, 8H)	

[a] H_{out} (d, J = 6.8−7.7 Hz, 8H), H_{in} (d, J = 6.8−7.7 Hz, 8H). The signals for the DBU•H^+ in the stock solution are as follows: 3.47 (m, 2H), 3.23 (m, 4H), 2.72 (m, 2H), 1.78 (m, 2H), 1.67 (m, 2H), 1.51 (m, 4H). [b] ^{1}H NMR spectrum recorded at 333 K. [c] Other signals overlap with DBU•H^+. [d] ^{1}H NMR spectrum recorded at 313 K.

plate ratios determined for the formation of carceplex **2a**•guest.[26] Reevaluation of the force field parameters should improve these correlations thereby honing the force fields used. The insight gained from the computations will also aid in the development of new self-assembling structures. Thus, a combination of experiment and computation should increase our knowledge of noncovalent interactions, which are instrumental to the formation of so many natural and nonnatural assemblies.

Experimental Section

General Experimental. Nitrobenzene and NMP were stirred over BaO for 24 h, distilled under reduced pressure, and stored under N_2 over 4 Å molecular sieves prior to use. All other commercially available reagents were used as purchased without further purification unless stated otherwise. ^{1}H NMR spectra were recorded on a Bruker WH-400 spectrometer in $CDCl_3$ at ambient temperature with the residual ^{1}H as a reference (7.24 ppm), or in nitrobenzene-d_5 with the residual ^{1}H's as references (7.50, 7.67, 8.11 ppm). ESI mass spectra were recorded on a SCIEX API 300 triple quadrupole mass spectrometer in the negative ion mode.

Crystal Structure of Complex 3b•Pyrazine. Crystals were grown by dissolving tetrol **1b** (0.11 mmol), DBU (0.22 mmol), and excess pyrazine (0.91 mmol) in nitrobenzene (8.0 mL) and letting the mixture stand in a closed vial for 30 days. A yellow prism-shaped crystal of dimensions 0.3 × 0.5 × 0.5 mm was mounted in a glass capillary. The asymmetric unit consists of $^1/_4$ of two crystallographically independent pyrazine complexes ($^1/_4$ × 2 × 2 bowls•pyrazine), two DBU•H^+ ions, one nitrobenzene, and two water molecules. The pyrazine guest molecule sits on a 4-fold axis and is thus disordered. Crystal data: tetragonal *P*4*cc* (no. 103); $a = b = 22.661(3)$ Å, $c = 30.209(2)$ Å; $V = 15512(2)$ Å^3; formula unit = $[C_9H_{17}N_2]_4^+$-$[C_{76}H_{64}N_2O_{24}]^{4-}$•$2C_6H_5NO_2$•$4H_2O$ with $Z = 4$; racemic; FW = 2320.61; $F(000) = 4936$; μ(Cu Kα) = 6.0 cm^{-1}; λ(Cu Kα) = 1.54178 Å; ρ_{calc} = 0.99 g/cm^3; t = 21 °C; 9337 reflections collected ($2\Theta_{max} = 130.0°$). Final full-matrix least-squares refinement (on F^2) based on 4426 unique reflections converged with 791 variable parameters and 928 restraints. Non-hydrogen atoms were refined anisotropically, hydrogen atom positions were calculated. $R(F) = 0.1130$ for 2018 $F_o > 4\sigma(F_o)$; GooF-(F^2) = 1.047; $\Delta\rho_{max} = 0.44$ e$^-$/Å^3, $\Delta\rho_{min} = -0.36$. All measurements were made on a Rigaku AFC6S diffractometer and the data analysis was performed with the program package teXsan and the program SHELXL-93.[28]

General Procedure for Determining the $t_{1/2}$ for Decomplexation of Pyrazine from Complex 3b•Pyrazine. The ^{1}H NMR spectrum of a mixture of tetrol **1b** (2.89 mM), DBU (6.1 mM), and pyrazine (1.45 mM) was recorded at 273 K in $CDCl_3$. Excess dioxane-d_8 (145 mM) was added to this sample and spectra were recorded as a function of time. The decrease in the concentration of complex **3b**•pyrazine was measured by integration of the unique host signals. A plot of ln[complex **3b**•pyrazine] versus time gives the approximate rate constant ($k_d = 1.2 \times 10^{-2}$ min^{-1}) for the decomplexation of pyrazine from this complex (Figure 7). Thus, the decomplexation was first order in complex **3b**•pyrazine, with a $t_{1/2}$ of 59 min. Only the initial rate is used (first five data points) to estimate k_d because as equilibrium approaches, the plot becomes nonlinear.

To establish equilibrium for relative binding studies, samples were typically equilibrated at the appropriate temperature for at least five times the half-life for the decomplexation of pyrazine (from the slowest complex if two hosts were in competition). This method for determining the time necessary for equilibration was found to correlate with simply recording the ^{1}H NMR of the samples, repeatedly until no change was observed. Pyrazine was shown to have the slowest half-life for decomplexation from complex **3b**•pyrazine ($t_{1/2}$ of 21 h) relative to complex **3b**•1,4-dioxane ($t_{1/2}$ of 4.2 h) and complex **3b**•DMSO ($t_{1/2}$ of 1 h) at 253 K in $CDCl_3$. Pyrazine (5 equiv) was used for displacing 1,4-dioxane and DMSO in complexes **3b**•1,4-dioxane and **3b**•DMSO, respectively.

General Procedure for Determination of K_{rel}'s for Complex 3b•Guest in $CDCl_3$. Tetrol **1b** (19.0 mg, 0.0289 mmol) was weighed into a 10.0 mL volumetric flask. To this were added 2.1 equiv of DBU (9.3 μL, 0.059 mmol) and the flask was filled to volume with $CDCl_3$. 4 Å molecular sieves (ca. 0.3 mg) and 500 μL of the above stock solution were added to ^{1}H NMR tubes: Stock solutions of the guests were added to each sample. ^{1}H NMR samples were prepared such that complex **3b**•guest 1:complex **3b**•guest 2 were ∼1:1 and the total amount of free species was less than 15% of the total host. The K_{rel}'s were determined by integration of the unique signals (H_p, H_{out}, H_{in}, and guest; see tetrol **1**, Scheme 1, for assignments) of the host and/or guest in each complex. See Table 3 for ^{1}H NMR assignments of complex **3**•guest.

The relative stability constants for complex **3b**•guest at 283, 313, and 323 K in $CDCl_3$ were determined in the same manner as described above. In all cases equilibration was achieved within 20 min. The moderate exchange rate (i.e., intermediate between fast and slow on the ^{1}H NMR time scale) of complex **3b**•benzene and complex **3b**•acetone at 323 K prevented the determination of K_{rel} for these complexes at this temperature. Complex **3b**•DMSO and complex **3b**•pyridine were broadened at 323 K but were still in slow exchange on the ^{1}H NMR time scale. The K_{rel}'s determined at 253 and 273 K were run as above except the ^{1}H NMR samples were equilibrated in a

(28) (a) Corporation, M. S. *teXsan. Single-Crystal Structure Analysis Software*; Version 1.7. MSC ed.; Corporation, M. S., Ed.: 3200 Research Forest Drive, The Woodlands, TX 77381, 1995. (b) Sheldrick, G. M. *SHELXL-93. Program for the Refinement of Crystal Structures.*; Sheldrick, G. M., Ed.: University of Göttingen, Germany, 1993.

constant-temperature bath over 48 and 16 h, respectively, prior to recording their ^{1}H NMR spectra.

General Procedure for Determination of K_{rel}'s for Complex 3b•Guest in Nitrobenzene-d_5. Tetrol **1b** (15.9 mg, 0.0218 mmol) was weighed into a 5.00 mL volumetric flask. To this were added 2.1 equiv of DBU (7.6 μL, 0.046 mmol) and the flask was filled to volume with nitrobenzene-d_5. 4 Å molecular sieves (ca. 0.3 mg) and 450 μL of the above stock solution were added to each ^{1}H NMR tube; all guests were added from stock solutions. ^{1}H NMR samples were prepared such that complex **3b**•guest 1:complex **3b**•guest 2 were ~1:1 and the total amount of free species was less than 1% of the total host. The K_{rel}'s were determined by integration of the unique signals of the host (e.g., H_p, H_{out}, H_{in}) and/or guest in each complex. See Table 4 for ^{1}H NMR assignments (a detailed discussion of the more complicated spectra will be reported elsewhere, along with a series of related complexes). For determination of the relative stability constants for NMP, $CHCl_3$, DMA, and 1,3-dioxane, 4.1 equiv of DBU were used.

The relative stability constants for complex **3b**•guest at 293, 303, 313, 323, and 333 K in nitrobenzene-d_5 were performed in the same manner as described above. Samples were equilibrated for 2 days in a constant-temperature bath prior to data acquisition. The moderate exchange rate of complex **3b**•1,3-dioxane, complex **3b**•DMA, complex **3b**•$CHCl_3$, and complex **3b**•NMP at temperatures above 313 K prevented the determination of their K_{rel} above 313 K. Equilibration of complex **3b**•1,3-dioxane, complex **3b**•DMA, complex **3b**•$CHCl_3$, and complex **3b**•NMP was achieved within 20 min at 313 K; thus, these four samples were only equilibrated in the spectrometer prior to data acquisition at 313 K.

Acknowledgment. We thank NSERC of Canada for generous funding. R.G.C. thanks NSERC and UBC for graduate fellowships. Acknowledgment is made to the donor of the Petroleum Research Fund, administered by the ACS, for partial funding. We thank Don Douglas and Bruce Collings for performing the electrospray mass spectrometry.

Supporting Information Available: Crystallographic information, tables of positional and thermal parameters, and a table of ESI signals (16 pages, print/PDF). See any current masthead page for ordering information and Web access instructions.

JA980081N